Dynamic Performance Testing of Excluded Spectra Range of Band-Stop-Filter

Gwanggil Jeon

Department of Embedded Systems Engineering, Incheon National University
12-1 Songdo-dong, Yeonsu-gu, Incheon 406-772, Korea
gjeon@incheon.ac.kr

Abstract

This paper studies about band-stop-filter which attenuates certain areas, and passes very high and very low band of frequencies. We study the influence of excluded spectra range by evaluating MSE and PSNR performance. Simulation results confirm that accepting more high frequency energy improves image details, and accepting more low frequency energy enriches image intensities.

Keywords: *band-pass-filter, band-stop-filter, digital image, frequency domain, spectra*

1. Introduction

The low-pass, high-pass, band-pass, and band-stop filtering processes are basic operations, which can be in the domains of spatial or frequency [1]. In this paper, we apply frequency domain band-pass-filter and evaluate the performance according to the range of spectrum [2]. The low-pass-filter is also known as filters for blurring or smoothing process, while the high-pass-filter is known as edge extraction. The most straightforward low-pass-filter process is average filter which average of neighbor pixels for its result pixel and the result pixel replace the original pixel. In image processing, a band-stop-filter is a filter that approves most frequencies without any changing, but attenuates those in a certain range to very low levels. Thus, this is opposite operation of a band-pass-filter. A good example of band-stop-filter is the notch filter which only passes narrow stopband [3].

Frequency domain filters operate an image in the frequency domain. First of all, the image is transformed by some kernel (usually Fourier transform), multiplied with the filter function (average, low-pass-filter, high-pass-filter, band-pass-filter, *etc.*) and then re-transformed into the spatial domain. Normally, weakening low frequencies intensifies the edges and weakening high frequencies makes images blur.

In this paper, we investigate the influence between excluded spectra range and the image performance. The paper is divided as follows. In Section 2, Fourier transform is described. The simulation results are presented in Section 3. Finally, in Section 4, we present our conclusions.

2. Fourier transform

The Fourier transform was invented by Joseph Fourier, which is a mathematical transform with many applications in physics, engineering, and image processing. Fourier transform is a crucial image processing method which is employed to decompose an image into its kernels, sine and cosine components [4-6]. The output of the Fourier transform shows the image in the frequency domain, where the intensity represents the power of its kernels [7-28]. This Fourier transform can be used in numerous image applications such as filtering, analysis, compression, reconstruction and restoration. Since we are only dealing with digital images, we only study the case of discrete Fourier transform (DFT). The DFT is the decimated Fourier transform, thus DFT does not include all image frequencies, while the DFT is only a group of components which must meet the condition: the number of components is large enough to entirely depict the spatial domain image. Let us assume an image with size $M \times M$, then 2D DFT is described by:

$$F(u,v)=\frac{1}{M^2}\sum_{x=0}^{M-1}\sum_{y=0}^{M-1} f(x,y)\, e^{-j2\pi\left(\frac{ux}{M}+\frac{vy}{M}\right)} \quad (1)$$

where $f(x,y)$ is an image in the spatial domain. The exponential term is the basis function pointing out each component $F(u,v)$ in the Fourier domain. Equation (1) is explained as follows. Each point $F(u,v)$'s intensity is computed by multiplying the image in spatial domain with the matching basis function and adding the results up. Two basis functions are sine wave and cosine wave with expanding frequencies. In other words, $F(0,0)$ stands for the DC energy of the image which tells the average intensities. $F(M-1,M-1)$ stands for the highest frequency. The inverse Fourier transform is described as Eq. (2).

$$f(x,y)=\frac{1}{M^2}\sum_{u=0}^{M-1}\sum_{v=0}^{M-1} F(u,v)\, e^{j2\pi\left(\frac{ux}{M}+\frac{vy}{M}\right)} \quad (2)$$

3. The Effect of Excluded Spectra Range of Band-stop-filter

To evaluate the effect of excluded spectra range, we made an ideal band-stop matrix, which is binary matrix *bm* defined by:

$$\mathcal{F}^{-1}(F(u,v)\cdot bm) \quad (3)$$

Figure 1(a) is the Fourier transformed image of Baboon, and the circle in Figure 1(b) is matrix *bm*, with range=50. Then, the inverse Fourier transform (*Φ*) of the component-wise multiplication of *F*(*u*,*v*) and *bm* is the result we obtain.

(4)

Figure 1(c) shows the result image after we apply filter in Eq. (4) to an original Baboon image.

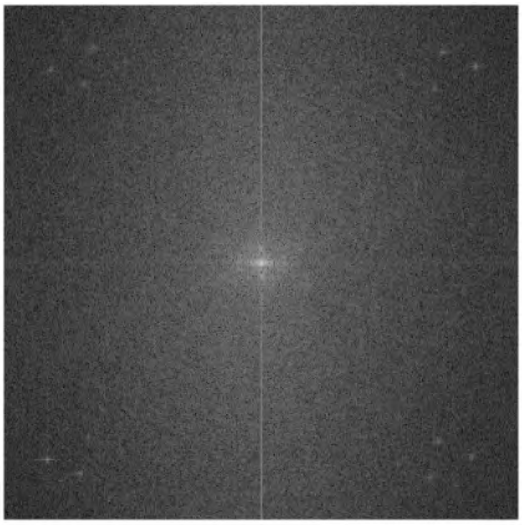

(a)

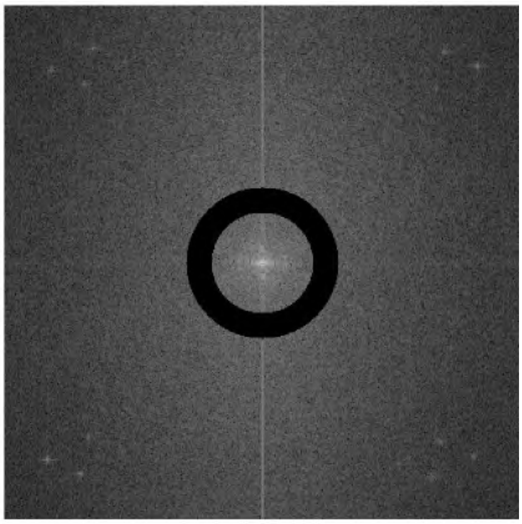

(b)

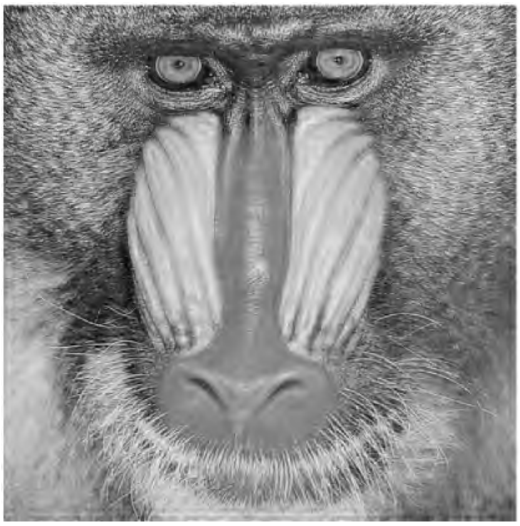

(c)

Figure 1. (a) Original Baboon image's DFT image, (b) DFT image's ideal band-stop-filtered image (range=50), (c) ideally filtered Baboon image

4. Performance investigation of excluded spectra range

In this section, we conducted experiments on 12 standard still images with the size of 512×512. They are Airplane, Baboon, Barbara, Boat, Finger, Girl, Lena, Man, Milkdrop, Peppers, Toys, and Zelda. To obtain PSNR and MSE performances according to the excluded spectra range, we evaluated the performance when 0≤range≤250, with the step size of 25. Figure 2 shows the MSE results according to the excluded spectra range 0, 25, 50, 75, 100, 125, 150, 175, 200, 225, and 250. Table 1 shows the PSNR results according to the excluded spectra range.

Figures 3-5 show the band-stop-filtered result images of Airplane, Girl, and Barbara. As we expected, when we removed low frequency energy we only obtained edge images as shown in Figure 3(a) and Figure 4(a). On the other hand, when we remove high frequency energy, we obtained blurred images.

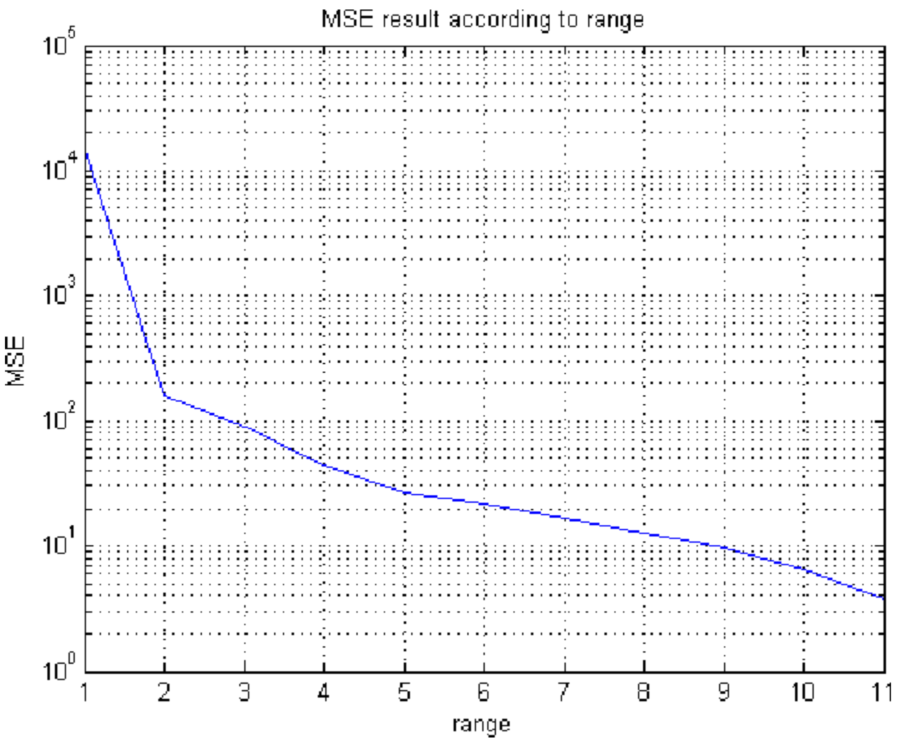

Figure 2. MSE results according to the spectra range

Table 1. Average PSNR according to the excluded spectra range

Range	0	25	50	75	100	125	150	175	200	225	250
Air	3.28	24.58	28.72	31.89	34.99	37.23	39.44	41.71	43.25	44.09	46.90
Bab	6.53	26.90	28.11	28.45	29.07	29.82	30.50	31.61	32.56	33.16	35.49
Bar	6.76	26.58	31.52	34.22	34.73	30.24	30.36	30.94	32.68	38.04	42.86
Boat	6.04	25.83	28.58	30.89	33.44	35.30	37.29	38.64	39.85	40.10	42.49
Finger	8.04	24.18	22.27	26.99	30.11	33.12	36.44	39.57	41.57	43.24	44.99
Girl	5.62	27.97	30.41	35.98	38.89	41.92	44.31	45.64	47.27	47.97	49.88
Lena	6.20	26.61	31.05	33.54	36.34	38.92	40.56	42.64	44.20	45.07	47.13
Man	8.62	24.70	28.42	30.68	32.30	33.57	34.72	35.48	36.20	36.72	38.22
Milk	7.34	28.36	34.82	37.77	40.44	42.81	44.44	45.18	45.82	46.42	49.25
Pepper	6.38	26.34	31.80	35.19	37.75	39.39	40.78	41.98	42.77	42.56	44.10
Toys	6.98	25.30	29.70	32.38	35.59	38.25	39.68	41.03	42.14	44.13	47.01
Zelda	7.22	29.87	35.31	38.04	41.22	44.01	46.02	47.21	48.37	48.69	50.95
Avg.	6.58	26.43	30.06	33.00	35.41	37.05	38.71	40.14	41.39	42.52	44.94

(a)

(b)

(c)

(d)

(e)

(f)

Figure 3. (a) Band-stop-filtered image of Airplane image with excluded spectra range=0, (b) excluded spectra range=25, (c) excluded spectra range=50, (d) excluded spectra range=75, (e) excluded spectra range=100, (f) excluded spectra range=125

(a)

(b)

(c)

(d)

(e)

(f)

Figure 4. (a) Band-pass-filtered image of Girl image with excluded spectra range=0, (b) excluded spectra range=25, (c) excluded spectra range=50, (d) excluded spectra range=75, (e) excluded spectra range=100, (f) excluded spectra range=125

Figure 5. (a) Band-pass-filtered image of Barbara image with excluded spectra range=0, (b) excluded spectra range=25, (c) excluded spectra range=50, (d) excluded spectra range=75, (e) excluded spectra range=100, (f) excluded spectra range=125

5. Conclusions

The band-pass-filter attenuates low and high frequency areas, and only passes a middle range band of frequencies. The band-pass-filter can be adopted to intensify details by stopping low frequencies. In this paper, we dealt with ideal band-stop-filter and evaluated its performance by excluding certain frequency area.

Acknowledgements

This work was supported in part by the National Science Foundation of China (NSFC) under Grant 61001100, 61077009.

References

[1] M. Petrou and C. Petrou, "Image Processing: The Fundamentals", Wiley, Amsterdam, **(2010)**.
[2] R. C. Gonzalez and R. E. Woods, "Digital Image Processing", Second Edition, Prentice-Hall, **(2002)**.
[3] K. K. Sundaram and V. Ramachandran, "Analysis of the coefficients of generalized bilinear transformation in the design of 2-D band-pass and band-stop filters and an application in image processing", in Proc. Canadian Conference on Electrical and Computer Engineering, **(2005)**, pp. 1233-1236.
[4] V. Namias, "The fractional order Fourier transform and its application to quantum mechanics", J. Inst. Math. Applicat., vol. 25, **(1980)**, pp. 241-265.
[5] L. B. Almeida, "The fractional Fourier transform and time-frequency representation", IEEE Trans. Signal Processing, vol. 42, **(1994)**, pp. 3084-3091.
[6] H. M. Ozaktas, Z. Zalevsky and M. A. Kutay, "The Fractional Fourier Transform with Applications in Optics and Signal Processing", Wiley, **(2000)**.
[7] M. Anisetti, C. A. Ardagna, E. Damiani, F. Frati, H. A. Müller and A. Pahlevan, "Web Service Assurance: The Notion and the Issues", Future Internet, vol. 4, no. 1, **(2012)**, pp. 92-109.
[8] M. Anisetti, C. A. Ardagna, V. Bellandi, E. Damiani, M. Döller, F. Stegmaier, T. Rabl, H. Kosch and L. Brunie, "Landmark-assisted location and tracking in outdoor mobile network", Multimedia Tools Appl., vol. 59, no. 1, **(2012)**, pp. 89-111.
[9] M. Anisetti, C. A. Ardagna, E. Damiani and J. Maggesi, "Security certification-aware service discovery and selection", SOCA, **(2012)**, pp. 1-8.
[10] M. Anisetti, C. A. Ardagna and E. Damiani, "A Low-Cost Security Certification Scheme for Evolving Services", ICWS, **(2012)**, pp. 122-129.
[11] M. Anisetti, C. A. Ardagna, V. Bellandi, E. Damiani and S. Reale, "Map-Based Location and Tracking in Multipath Outdoor Mobile Networks", IEEE Transactions on Wireless Communications, vol. 10, no. 3, **(2011)**, pp. 814-824.
[12] M. Anisetti, C. A. Ardagna, V. Bellandi, E. Damiani and S. Reale, "Advanced Localization of Mobile Terminal in Cellular Network", IJCNS, vol. 1, no. 1, **(2008)**, pp. 95-103.
[13] C.-T. Hsieh, Y.-K. Wu and K.-M. Hung, "Hybrid Watermarking Scheme for Halftone Images", International Journal of Advanced Science and Technology, **(2008)**, pp. 9-20.
[14] R. Adipranata, E. Cherry, G. Ballangan and R. P. Ongkodjojo, "Fast Method for Multiple Human Face Segmentation in Color Image", International Journal of Advanced Science and Technology, **(2009)**, pp. 19-32.
[15] D. Bhattacharyya, A. Roy, P. Roy and T.-h. Kim, "Receiver Compatible Data Hiding in Color Image", International Journal of Advanced Science and Technology, **(2009)**, pp. 15-24.
[16] M. Drahanský, "Realization of Experiments with Image Quality of Fingerprints", International Journal of Advanced Science and Technology, **(2009)**, pp. 79-88.
[17] B. V. Ramana Reddy, A. Suresh, M. Radhika Mani and V.Vijaya Kumar, "Classification of Textures Based on Features Extracted from Preprocessing Images on Random Windows", International Journal of Advanced Science and Technology, **(2009)**, pp. 9-18.
[18] W. Wu, Z. Liu and X. He, "Learning-based super resolution using kernel partial least squares", Image Vision Comput., vol. 29, **(2011)**, pp. 394-406.
[19] W. Wu, Z. Liu, W. Gueaieb and X. He, "Single-image super-resolution based on markov random field and contourlet transform", J. Electron. Imaging, vol. 20, 023005, **(2011)**.
[20] W. Wu, Z. Liu and D. Krys, "Improving laser image resolution for pitting corrosion measurement using markov random field method", Autom. Constr., vol. 21, **(2012)**, pp. 172-183.
[21] W. Wu, Z. Liu, M. Chen, X. Yang and X. He, "An automated vision system for container-code recognition", Expert Systems with Applications, vol. 39, **(2012)**, pp. 2842-285.

[22] W. Wu, X. Yang and X. He, "Handwritten numeral recognition by model reconstruction based on manifold learning", in: The 2007 International Conference on Information Computing and Automation (ICICA'07), **(2007)**.
[23] J. Wu, C. Liang, J. Han, Z. Hu, D. Huang, H. Hu, Y. Fang and L. Jiao, "A Two-Stage Lossless Compression Algorithm for Aurora Image Using Weighted Motion Compensation and Context-Based Model", Optics Communications, vol. 290, **(2012)** October 22, pp. 19-27.
[24] Y. Fang, J. Wu, and B. Huang, 2D sparse signal recovery via 2D orthogonal matching pursuit. Science China: Inf. Sci., 55: 889-897, (**2012**).
[25] J. Wu, T. Li, T. -J. Hsieh, Y. -L. Chang and B. Huang, Digital Signal Processor-based 3D Wavelet Error-resilient Lossless Compression of High-resolution Spectrometer Data. Journal of Applied Remote Sensing, Vol. 5, 051504, November 28, (**2011**).
[26] A. Paul, J. Wu, J. -F. Yang and J. Jeong, "Gradient-based edge detection for motion estimation in H.264/AVC", IET Image Processing, vol. 5, no. 4, **(2011)**, pp. 323–327.
[27] J. Wu, J. Huang, G. Jeon, J. Jeong and L. C. Jiao, "An adaptive autoregressive de-interlacing method", Optical Engineering, vol. 5, no. 50, 057001, **(2011)**.
[28] J. Wu, A. Paul, Y. Xing, Y. Fang, J. Jeong, L. Jiao and G. Shi, "Morphological dilation image coding with context weights prediction", Signal Processing: Image Communication, vol. 25, no. 10, **(2010)**, pp. 717-728.

Authors

Gwanggil Jeon received his BS, MS, and PhD (summa cum laude) degrees in Department of Electronics and Computer Engineering from Hanyang University, Seoul, Korea, in 2003, 2005, and 2008, respectively.

From 2008 to 2009, he was with the Department of Electronics and Computer Engineering, Hanyang University, from 2009 to 2011, he was with the School of Information Technology and Engineering (SITE), University of Ottawa, as a postdoctoral fellow, and from 2011 to 2012, he was with the Graduate School of Science & Technology, Niigata University, as an assistant professor. He is currently an assistant professor with the Department of Embedded Systems Engineering, Incheon National University, Incheon, Korea. His research interests fall under the umbrella of image processing, particularly image compression, motion estimation, demosaicking, and image enhancement as well as computational intelligence such as fuzzy and rough sets theories. He was the recipient of the IEEE Chester Sall Award in 2007 and the 2008 ETRI Journal Paper Award.